Check for updates

Chemistry
Europe
European Chemical
Societies Publishing

Metal-free phthalimide-labeled peptide nucleic acids for electrochemical biosensing applications

Mirko Magni[1,#] | Sergio Dall'Angelo[1,2,#] | Clara Baldoli[3] |
Emanuela Licandro[1] | Luigi Falciola[1] | Patrizia R. Mussini[1]

[1] Department of Chemistry, Università degli Studi di Milano - Via C. Golgi 19, Milano, Italy
(Email: s.dallangelo@abdn.ac.uk)

[2] Institute of Medical Sciences, University of Aberdeen, Aberdeen, Scotland, UK

[3] CNR- Institute of Chemical Sciences and Technologies (SCITEC), Milano, Italy

Correspondence
Mirko Magni, Department of Chemistry, Università degli Studi di Milano - Via C. Golgi 19, 20133 Milano, Italy.
Email: mirko.magni@unimi.it

[#]The two authors contributed equally

Abstract

Peptide nucleic acids (PNAs) are neutral mimics of natural DNA and RNA biopolymers that have caught the attention of researchers working on the identification of specific sequences of nucleobases in DNA/RNA strands. For this purpose, specific analytical protocols need to be developed to optimize the nucleic acid recognition ability of PNAs, exploiting both the high intrinsic affinity of PNA/DNA(RNA) couples as well as suitable markers, either linked to the PNA backbone or properly interacting with it in the working medium. In this context, the paper reports on phthalimide and 4-nitrophthalimide as two cheap, metal-free electroactive markers covalently bound to the pseudo-peptide backbone of a PNA decamer. After a preliminary characterization of the markers, as such and in PNA conjugates, attention has been moved toward the optimization of the detectability of the labeled PNA decamers in aqueous solutions. Exploiting the potentiometric stripping analysis on hanging mercury drop electrode it has been possible to reach satisfactory detection limits of ca. 10 nM avoiding the use of expensive transition metal complexes as labels and/or of co-reagents.
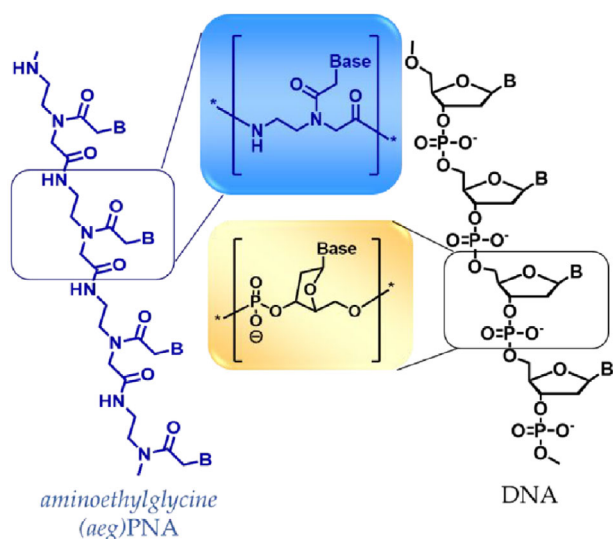
1 | INTRODUCTION

Peptide nucleic acids (PNAs) are artificial nucleic acid mimics whose structure is based on a neutral pseudo-peptide backbone, made of *N*-(2-aminoethyl)glycine units (Figure 1), that replaces the negatively charged sugar-phosphate chain of natural nucleic acids (DNA and RNA).[1,2] Nucleobases (adenine, guanine, cytosine, and thymine) are covalently bound to this backbone thus giving PNA the ability to recognize and bind in a very strong, highly specific, and selective manner complementary DNA or RNA sequences according to Watson–Crick base-pairing rules. PNAs are chemically stable towards a wide range of temperatures and pHs and, thanks to

their non-natural polyamide backbone, are not degraded by enzymes such as nucleases and proteases. Thanks to these properties, PNAs are ideal systems for the development of diagnostic platforms, being excellent probe candidates for the recognition of nucleic acid sequences. Applications spread from the development of innovative nucleic acid biosensors, and related diagnostic protocols, to the employment as tools in molecular biology and functional genomics.[3,4] More specifically, biosensors can be developed thanks to the ability of PNA to recognize specific (complementary) sequences of DNA and pick them up from a mixture of genes. If the PNA backbone is functionalized with a convenient active label,[5] its hybridization with its complementary nucleic acid can be detected and

2 of 12   **Electrochemical Science Advances**   RESEARCH ARTICLE
doi.org/10.1002/elsa.202100164

**Chemistry
Europe**
European Chemical
Societies Publishing

FIGURE 1   Neutral PNA versus negatively charged DNA backbone

converted into an analytical signal (such as electrochemical, fluorescent, radioactive, or other ones).

Focusing on the possibility to implement PNAs as probes in affinity bio-electrochemical sensors for nucleic acids, two main experimental protocols have been proposed.[6,7] A first one, termed "label-free," exploits either the intrinsic features of PNA molecules to obtain an analytical signal (e.g., the redox capacities of nucleobases, the electrical negative charge of DNA strand) or the redox response of an active compound dissolved in the working solution. A second approach requires the use of a covalently linked electroactive marker (i.e., an "external label"). Recently, these strategies have been combined with different electrode substrates, including even a paper-based electrochemical cell.[8] In the past, our group already explored the field of PNA-labeling[9] studying the electrochemical properties of a transition metal-based electroactive marker (ferrocene), selected for the intrinsic chemical and electrochemical reversibility of its electrically-induced Fe^{2+}/Fe^{3+} redox conversion on the glassy carbon (GC) electrode.

In the present work, we propose two innovative metal-free labels for PNA oligomers, based on the phthalimide unit (Figure 2). The phthalimide was chosen thanks to the suitable feature of the electrochemical signal(s) associated with the reversible electroreduction(s) and to the easy conjugation to PNA. An extensive electrochemical characterization was performed by a systematic approach, that is, from the isolated markers to their PNA conjugates, affording a neat rationalization of the relationship between molecular structure, redox potential window, and detection limit, the latter fundamental for assessing any analytical application of the labeled PNA oligomers as a tool

for DNA sequence detection. The investigation covered the six-molecule series reported in Figure 2A, including:

a. the pristine marker molecules, phthalimide **P** and nitrophthalimide **NP**;
b. their *N*-Boc-lysine conjugates, **P$_{Lys}$** and **NP$_{Lys}$** (Boc = *tert*-butyloxycarbonyl protecting group);
c. **P$_{Dec}$** and **NP$_{Dec}$**, i.e. their conjugates via the modified-lysine linker to an aminoethylglycine PNA (*aeg*PNA) decamer, featuring the GTAGATCACT nucleobase sequence (G = guanine, T = thymine, A = adenine, C = cytosine) as shown in Figure 2B.
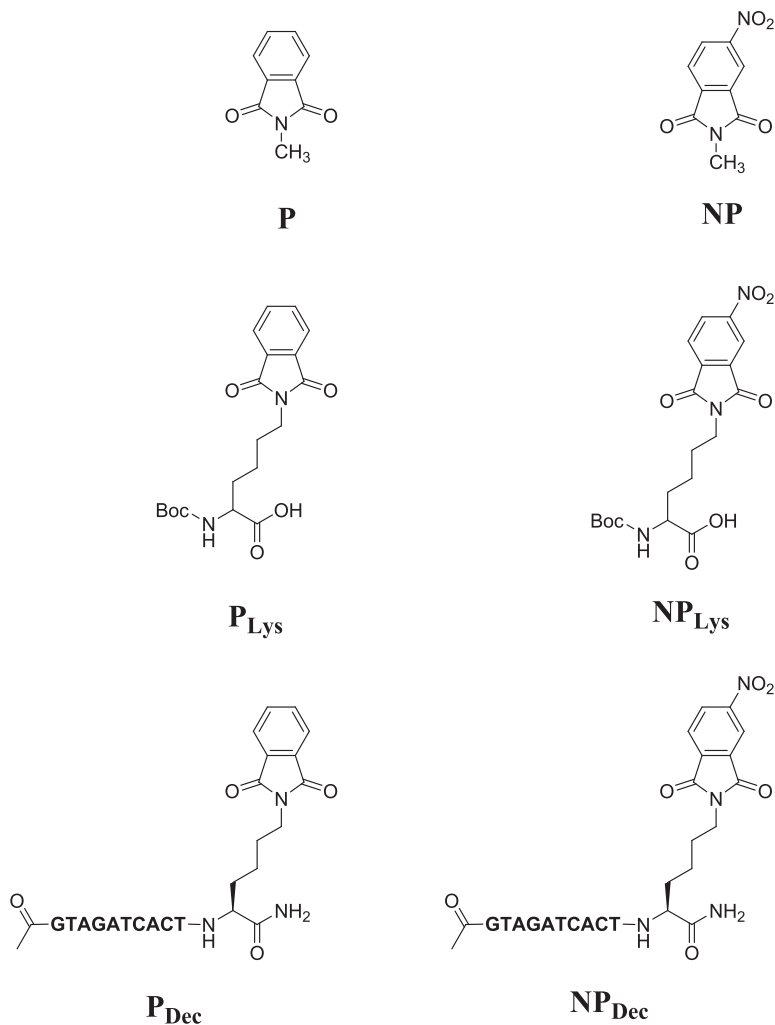
The study has been carried out on two electrode materials that offer different surface properties, and in two media of different proticity. In particular:

- GC, providing a reference material for studying the intrinsic molecule reactivity without specific surface interactions, and Hg (as hanging drop mercury electrode, HDME), promoting both specific DNA adsorption[10] and PNA adsorption[11–13];
- *N,N*-dimethylformamide (DMF), as an aprotic organic solvent, and water. The latter is of particular interest because it represents the election solvent for practical application in the development of sensors and biosensors able to detect specific DNA nucleotide sequences;
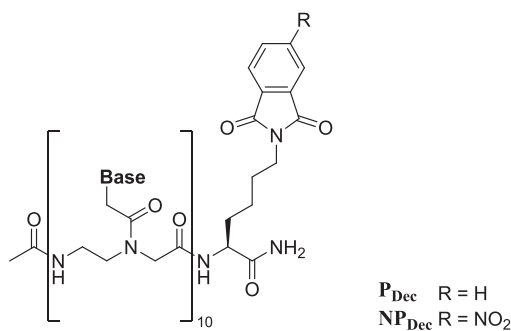
Looking for the best detection limit for PNA decamers, potentiometric stripping analysis (PSA) was found to be the most effective approach. PSA is a chronopotentiometric technique in which oxidation/reduction of preconcentrated species on an electrode surface is followed by monitoring the variation of the working potential as a function of time,[14] obtaining a potential (E) versus time (t) chronopotentiogram. In the resulting sigmoidal step curve, the potential tends to reach the dynamic equilibrium value accounted for by the Nernst equation (being a function of nature and concentration of the redox active species involved) with a speed directly related to the applied current intensity. The corresponding *differential peak plot*, dt/dE versus E, is commonly more useful than the sigmoidal curve, since the quantitative information, that is, analyte concentration, is proportional to the time required for the complete dissolution of accumulated species, easily assessable by the *transition time* parameter (τ) obtained by integration of the peak.

In the interest of clarity, there is a literature debate regarding the correct definition of the aforementioned electroanalytical technique, depending on the nature of the driving force responsible for the stripping stage.[15] Historically, the term PSA was originally used when a chemical redox species triggers the stripping stage, while

3 of 12   **Electrochemical Science Advances**

RESEARCH ARTICLE
doi.org/10.1002/elsa.202100164

**Chemistry
Europe**
European Chemical
Societies Publishing

FIGURE 2 Upper panel (A): molecular structure of the six investigated molecules. Bottom panel (B): detailed structure of the *aeg*PNA decamers P_{Dec} and NP_{Dec} conjugated to the electrochemically active markers via the lysine linker

chronopotentiometric stripping analysis, or even *constant current* stripping analysis , has been proposed later by some Authors when current is used to trigger the same process. Hereafter, we adopt the general term PSA to indicate the technique exploited in this study, which implies the application of a constant cathodic current to reduce the adsorbed analyte.

2 | MATERIALS AND METHODS

The two electrochemical markers as single molecules (**P** and **NP**) are commercially available (*N*-methyl phthalimide, Aldrich, 98%; 2-methyl-5-nitro-isoindole-1,3-dione, **NP**, Aldrich). Conversely, the corresponding four conjugates P_{Lys}, NP_{Lys}, P_{Dec}, and NP_{Dec} were synthesized de
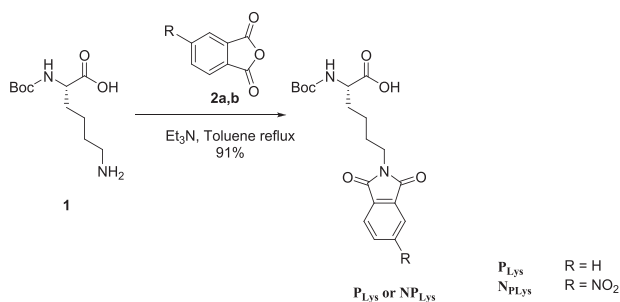
SCHEME 1   Synthesis of *N*-Boc-lysine conjugates

novo as reported below. Details of their preparation and characterization are provided in the Supporting Information file.

2.1 | Synthesis and chemical characterization

Compounds P_{Lys} and NP_{Lys} were obtained in 91% yield by treatment of commercially available $N(\alpha)$-Boc-L-lysine **1** with the corresponding phthalic anhydride **2a** or **2b** in toluene in the presence of triethylamine as a base (Scheme 1).

In order to prepare the *aeg*PNA decamers P_{Dec} and NP_{Dec} lysine derivative P_{Lys} or NP_{Lys} were first linked to the MBHA resin **3** (Scheme 2 and Supporting Information) to give the corresponding P_{Lys} / NP_{Lys} functionalized resins **4a,b**. The synthesis of decamers P_{Dec} and NP_{Dec} was then completed using the standard solid-phase technique with a peptide synthesizer on a 20-μmol scale exploiting the *Boc*-chemistry[16] by the sequential addition of each *aeg*PNA monomer.

After the cleavage from the resin, each PNA decamer was isolated in 20% overall yield by precipitation at room temperature with diethyl ether. The crude P_{Dec} was pure enough to be used in the following electrochemical characterization, while the crude of NP_{Dec} was purified by HPLC equipped with a semipreparative reverse-phase column. MALDI-TOF and HRMS analysis confirmed the structures of either decamer (see Supporting Information).

2.2 | Electrochemical characterization

All the electrochemical experiments, both voltammetric and chronopotentiometric, were carried out in a small cell (operating with 3–4 cm^3 working solution) or in a larger conical one (10 cm^3). A GC (Amel, Italy; surface area 0.071 cm^2) or a hanging drop mercury electrode HDME (average surface area 0.042 cm^2) were used as working electrodes, a Pt wire as counter-electrode, and an aqueous saturated

calomel electrode (SCE) as a reference electrode. The latter was inserted into a jacket filled with a solution of the same electrolyte used in the cell and ensuring contact with the working solution via a glass joint, in order to avoid precipitation of the tested substrates within the SCE porous frit and to minimize KCl leakage into the working solution. The potentials have been subsequently referred to the reference redox couple $Fc^+|Fc$ (ferricinium|ferrocene) measured in similar conditions (0.476 V vs. SCE in pure DMF; 0.165 V vs. SCE in water), in order to facilitate comparison of results obtained in different solvents.[17] In the interest of clarity, the slight solubility of ferrocene in water is still sufficient to record a satisfactory, even if weak, CV signal that was employed for the estimation of the half-wave potential. The geometric area of the Hg drops at HDME was determined by mediating the weight of a suitable known number of equal drops of mercury obtained, at least, twice a day.

Experiments, performed in a solution well deaerated by bubbling nitrogen before the scans and keeping the gas flux over the surface during the measurements, were carried out using either a PGSTAT 12 potentiostat/galvanostat with the 663 VA Stand polarograph (Eco-Chemie, The Netherlands) or an Autolab PGSTAT 30 potentiostat/galvanostat (EcoChemie, The Netherlands) in combination with HDME WK2 (Institute of Physical Chemistry Polish Academy of Sciences, Warsaw, Poland) or GC electrode. Both potentiostats were interfaced with a PC by GPES software. The mother solutions of the six molecules analyzed were prepared using highly deionized water (Millipore Milli-Q$^\circledR$ system) or *N*,*N*-dimethylformamide (DMF, Sigma–Aldrich, ≥99.8%), according to their solubility.

The electrochemical diffusive analyses (cyclic voltammetry CV, differential pulse voltammetry DPV, square wave voltammetry SWV) were carried out in solutions containing a suitable concentration of the sample with 0.1 M potassium perchlorate (KClO$_4$, Sigma–Aldrich, ≥99%) as supporting electrolyte in DMF, and 0.5 M sodium perchlorate monohydrate (NaClO$_4$·H$_2$O, Baker Analyzed$^\circledR$) in water.

Staircase CVs were recorded with a 0.2 V/s scan rate (unless indicated) and 0.001 V step potential. With differential pulse techniques the working parameters were:

- for DPV: 0.05 s modulation time, 0.3 s interval time, 0.005 V step potential, modulation amplitude 0.050 V;
- for SWV: 100 Hz or 50 Hz frequency, 0.005 V step potential, 0.050 V amplitude.

The chronopotentiometric adsorptive experiments were carried out on the decamers only, following two different protocols (Chart 1): i) adsorptive potentiometric stripping
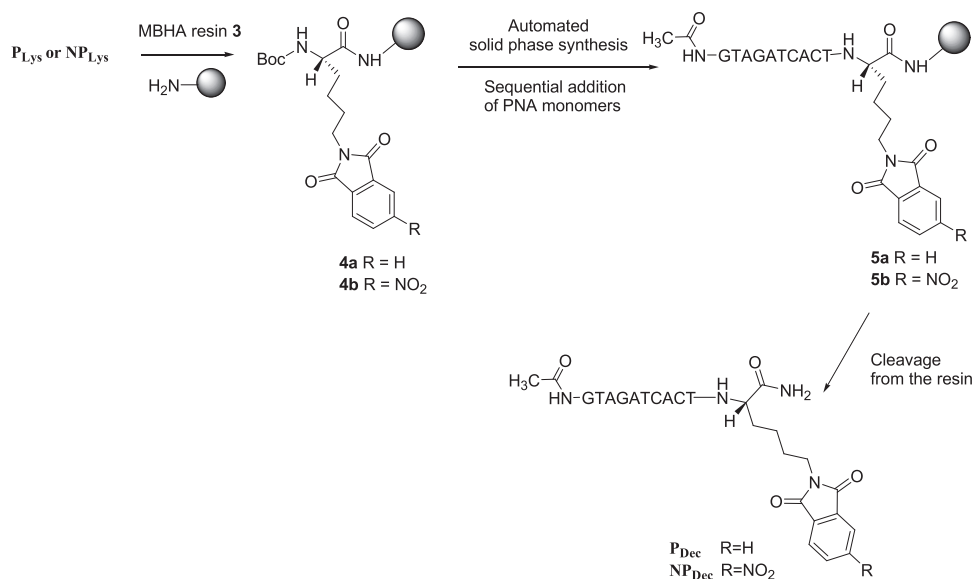
SCHEME 2 Synthesis of *aeg*PNA decamers P_{Dec} and NP_{Dec} on MBHA resin

analysis Ad-PSA (adsorption and stripping performed in the same solution) and ii) adsorptive *transfer* potentiometric stripping analysis AdT-PSA (adsorption and stripping performed in two different solutions).

Potentiometric stripping analyses were performed in aqueous solution with 0.2 M sodium chloride (NaCl, Fluka, ≥99.5%) as supporting electrolyte, buffered at pH 7 with 0.025 M sodium hydrogen phosphate plus sodium dihydrogen phosphate (Fluka, pH 7 buffer, 0.05 M in Na_2HPO_4 + NaH_2PO_4) to facilitate adsorption.[13,18] On the contrary, decamer stock solutions have been prepared in DMF, granting full solubility and therefore reproducible sampling. For the AdT experiments, the accumulation was carried out by carefully placing in contact the hanging Hg drop of the electrode with a 10 μl sample drop of PNA (in pH buffer) deposited on a Parafilm® sheet. After that, HDME was carefully dipped multiple times in MilliQ water to remove any residue and, finally, transferred into a cell containing 3.0 cm^3 of the aforementioned PNA-free solution. For the simpler Ad-PSA protocol, the deposition and stripping occur, without solution of continuity, in the same 3.0 cm^3 aqueous solution containing the sample (added as DMF solution), the supporting electrolyte (NaCl), and the pH buffer. Even with the Ad-PSA protocol, measures can be soundly referred to the aqueous medium, since the PNA stock solutions spiked into the aqueous background resulted in a maximum DMF/H_2O ratio of 0.03:1.

The PSA measurements were carried out with the following parameters: deposition potential set at 0 V versus SCE (or at open circuit potential for AdT-PSA), 60 s deposition time, 5 s equilibration time, 1 μA (cathodic) stripping current.
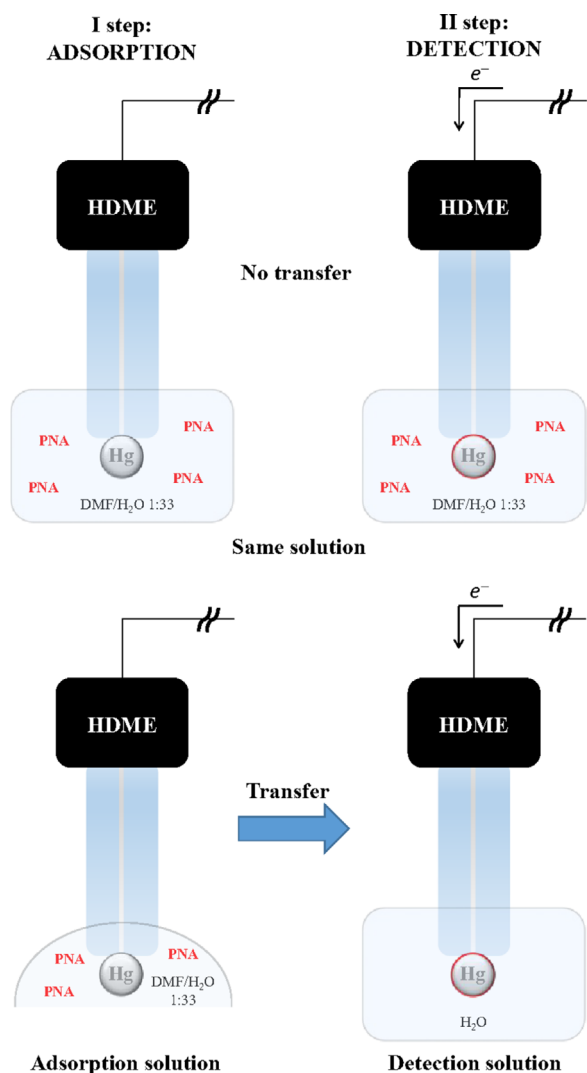
3 | RESULTS AND DISCUSSION

3.1 | Preliminary voltammetric investigation of the redox markers

The electronic properties of marker molecules as such (**P** and **NP**) and as lysine conjugates (P_{Lys} and NP_{Lys}) were preliminarily studied by CV and SWV in DMF on the GC electrode (Figure 3). All molecules have their first reduction peaks in a potential range that is not too extreme and in which no background signals are present.

3.1.1 | Phthalimide series

P features a single detectable peak at –1.92 V versus Fc$^+$|Fc, chemically and electrochemically reversible and monoelectronic (half-peak width ca. 0.057 V) corresponding to the reduction of phthalimide to the corresponding radical anion, stable in the absence of protons. A second reversible peak should be detectable in aprotic media at about –2.65 V versus Fc$^+$|Fc, that is, in the proximity of the GC negative operating limit, corresponding to dianion formation.[19,20] The scan was however inverted before such potential, since the peak would have been too extreme for the present applicative aim (*inter alia* it would be covered by the background reaction in an aqueous medium).

P_{Lys} exhibits a comparable CV pattern, but the reduction peak has remarkably lower chemical reversibility. Such feature can be attributed to an electrochemical-chemical (EC) mechanism, with a chemical step following the electron transfer(ET) one, promoted by the presence of an intramolecular in situ source, the -COOH group

6 of 12 | **Electrochemical Science Advances** | RESEARCH ARTICLE
doi.org/10.1002/elsa.202100164

**Chemistry
Europe**
European Chemical
Societies Publishing

CHART 1 Sketches of the two protocols adopted for the chronopotentiometric adsorptive experiments with PNA decamers (P_{Dec} and NP_{Dec}): Ad-PSA (top) and AdT-PSA (bottom)

of lysine. It can be assumed that the radical anion formed in the ET is protonated forming a hydroxyl radical species which itself inhibits the reversibility of the process and, on the other hand, provides an alternative chemical reaction pathway.[19,20] Actually, a similar loss in chemical reversibility is also observed upon small additions of acetic acid (Figure 3a). In both cases, the protonation of the radical anion generated at ca. −1.9 V versus $Fc^+|Fc$ is almost complete within ca. 3 s, considering the scan rate of the potential.

Moreover, the reduction peak of P_{Lys} is slightly shifted to a more positive potential (easier reduction) with respect to the free marker. Such an effect cannot be attributed to any direct electronic effect of the lysine moiety, being separated from the redox active core through an alkyl chain, preventing conjugation. The different alkyl substituent length seems insufficient as a justification, considering that alkyl chains have nearly constant Hammett parameters accounting for inductive effects.[21] Even simple acid/base effects should be ruled out by comparison with the **P** + acetic acid case (Figure 3a), resulting in no significant shift. However, it is worthwhile noticing that a positive shift of the reduction peak potential can be observed when the ET (a) is faster with respect to mass transfer and (b) results in a product undergoing a chemical follow-up process faster than mass transfer.[22] By the way, a positive shift of the reduction potential is also observed when the product is involved in an equilibrium, e.g. a coordination one, with $K >> 1$, or in a specific adsorption of the product on the electrode surface.[23] Something of the kind might also concern the P_{Lys} substrate, particularly considering the intramolecular availability of a carboxylic group able to react with the radical anion product and even located in a position suitable for internal coordination with it.
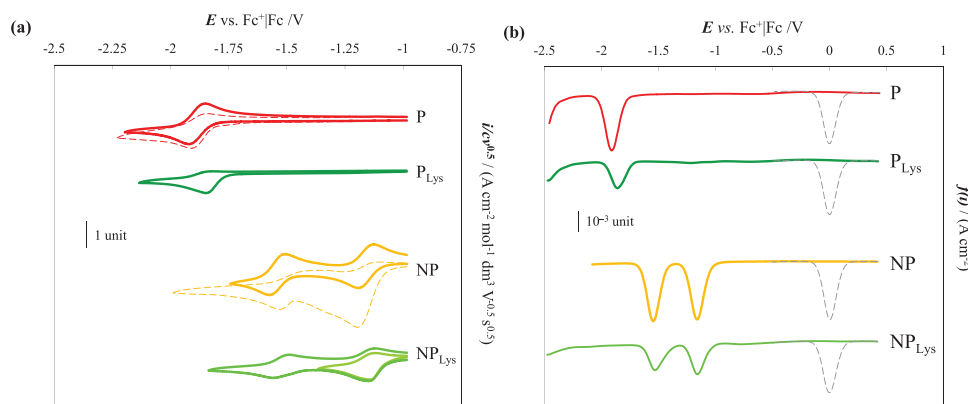
FIGURE 3 CV (a) and SWV (b) characteristics on GC electrode of the two marker molecules, **P** and **NP**, and of their lysine conjugates, P_{Lys} and NP_{Lys}, at $1.5 \cdot 10^{-3}$ M concentration in DMF with 0.1 M $KClO_4$ supporting electrolyte. CV: recorded at 0.2 V/s, dashed lines after addition of acetic acid 5:1 molar ratio. SWV: recorded at 0.25 V/s (50 Hz), grey dashed lines corresponding to equimolar ferrocene

3.1.2 | Nitro-phthalimide series

The NP series differs from the previous one by the presence of a nitro group on the phthalimide ring. This remarkably modifies the CV pattern, which now includes two peaks at much more positive potentials (-1.15 V versus $Fc^+|Fc$ and -1.57 V versus $Fc^+|Fc$, Figure 3), both conveniently exploitable for analytical purposes, attributable to subsequent electron transfers centered on the easier reducible $-NO_2$ functionality than the phthalimide moiety. Both peaks are both monoelectronic and chemically and electrochemically reversible, a pattern consistent with the reported general reactivity of nitroarenes in aprotic solvents.[24] In particular, while the first ET is likely to be associated with the formation of a stable radical anion localized on the nitro group, the second one is usually associated with dianion formation on the same site, albeit in our case the negative charge could also involve the phthalimide ring, being itself a reduction site. Another difference is the remarkable intensification of the first cathodic peak of **NP** by adding an excess of acetic acid as an external source of protons (Figure 3a), pointing to a multi-electron proton-coupled transfer process, unlike the simpler **P** case. Generally speaking, the addition of an organic acid brings to the appearance of a new positively shifted multi-electron peak, with respect to the monoelectronic one recorded in the aprotic medium, characterized by a three to four times higher peak current density.[25] Nonetheless, some acids do not produce this shift still preserving the peak current increase,[25] as occurred for the addition of 5 eq. of acetic acid to the **NP** solution. Even if no detailed mechanistic insight can be provided, this experimental evidence further points out that the redox center moves from the phthalimide moiety (**P** series) to the nitro group (**NP** series).

In the NP_{Lys} case, featuring a free acid group, chemical reversibility decreases, as in the P series (Figure 3). Nonetheless, the peak potential is almost invariant with respect to **NP**, unlike in the P_{Lys} case, which could be consistent with the above assumption concerning the difference in the redox centers involved in the first reduction process.

The intensities of the diffusive signals for **P** and **NP** are comparable with those of ferrocene added in equimolar quantity (Figure 3b), in agreement with the similar dimensions of the two markers with that of the reference diffusive redox probe. This experimental data further support the above-mentioned thesis of the monoelectronic nature of the ET processes that characterize the voltammetric pattern of the two markers. Reasonably, the current peak decreases with the increasing bulkiness and the presence of coordination elements, from free markers (N-methyl-phthalimide and N-methyl-4-nitrophthalimide) to

the lysine conjugates (P_{Lys} and NP_{Lys}, respectively), characterized by smaller diffusion coefficients. Nevertheless, currents remain to be detectable for analytical purposes (especially using SWV).
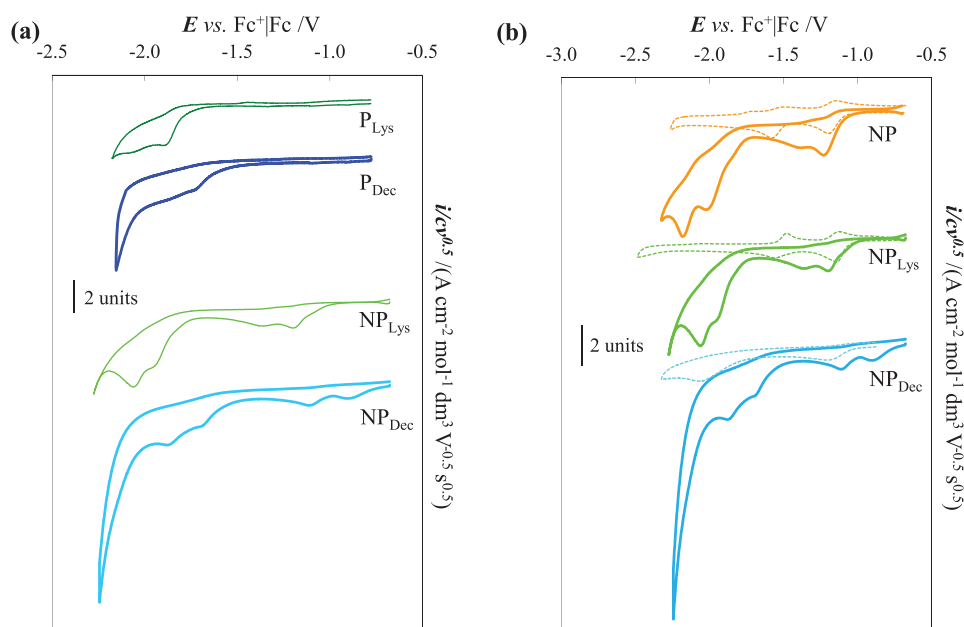
3.2 | Pre-applicative characterization of PNA decamers on HDME electrode

The preliminary characterizations on the GC electrode were then extended to assess the behavior of the labeled PNA decamers on the HMDE electrode, on account of the potential ability of mercury to strongly adsorb DNA and PNA material.[10–12] This feature affords a way to preconcentrate the PNA decamers enabling the application of a stripping technique, thus significantly lowering the limit of detection with respect to the diffusive pulse voltammetry techniques (like SWV), adopted in the preliminary study on GC.

The CV patterns of both labeled decamers on HDME are depicted in Figure 4a, together with those of the lysine conjugates, for sake of comparison. P_{Dec} exhibits two subsequent electron transfers at relatively negative potentials, partially superimposed to the background discharge. By comparison, the much more reducible nitro group should be responsible for the first two peaks of NP_{Dec}, followed by a second couple of peaks, which could involve the phthalimide ring. While the corresponding second couple of peaks for NP_{Lys} occur at more negative potentials than those related to phthalimide reduction in P_{Lys} (consistently with the presence of a negative charge on the nitro-bearing molecule), such an effect is less evident in the related decamers.

The peak intensities of both decamers are lower than the corresponding lysine conjugate ones, consistent with the higher steric hindrance and, hence, lower diffusion coefficients of the PNA molecules. Interestingly, both labeled decamers show peaks placed at potentials at least 120 mV more positive than the corresponding lysine conjugate, a shift that can be hardly correlated with any variation of the electronic effects between lysine and PNA conjugates. On the contrary, the explanation can be associated with the electrode material.

The effect of electrode material (i.e., GC versus Hg) was studied on the NP series (Figure 4b), its more positive peak potentials preventing any overlapping with the background signal (compare NP_{Dec} and P_{Dec} traces in Figure 4a). In the **NP** and NP_{Lys} cases, while only small potential differences are observed for the first peak (Figure 4b), their electrochemical patterns as a whole are significantly affected by moving from an ideally "inert" electrode surface (i.e., GC) to a surface potentially able

8 of 12   **Electrochemical Science Advances**

RESEARCH ARTICLE
doi.org/10.1002/elsa.202100164

Chemistry Europe
European Chemical
Societies Publishing

FIGURE 4   Left (a): normalized CV characteristics of labeled PNA decamers (thick lines) on Hg electrode. For sake of comparison, related lysine conjugates (thin lines) are also reported. Right (b): normalized CV patterns for the nitro series recorded on Hg (continuous lines) and on GC electrode (dashed lines). In all cases: DMF with 0.1 M KClO$_4$ supporting electrolyte, 0.2 V/s potential scan rate

to induce adsorption phenomena (i.e., Hg). Concerning the two subsequent electron transfers at the less negative potentials, the peak potential distance is significantly reduced on Hg accompanied by a net variation of their relative peak currents. Even if no additional studies have been performed (e.g., change in the potential scan rate), it is possible to tentatively explain all these variations in terms of a different mechanism (probably surface-mediated one) triggered by the Hg surface. Moreover, the reactivity at more negative potentials also changes, with the occurrence, inter alia, of well-defined subsequent ET processes centered on the aromatic ring (see also above). The significant positive shift, by moving from GC to Hg electrode (Figure 4b), of the first reduction peak observed only for **NP$_{Dec}$** could be explained in terms of some adsorption auxiliary effect by the nitrogen atoms of the nucleobases, as confirmed by the cited literature.[10–12] This additional experimental proof further confirms the potentiality of the Ad(T)PSA techniques for quantitative analysis purposes of PNA-bearing molecules.

3.2.1 | Effect of the aqueous medium

Since the possibility to use a mercury electrode in water would enable convenient applicative conditions for PNA biosensors, the voltammetric characterization was extended to the pure aqueous medium. As anticipated, due to solubility issues, any direct investigation through diffusive techniques is precluded for both PNA-decamers.

Therefore, **P$_{Lys}$** was selected as the best candidate for this study, in terms of compromise between solubility in water and structural similarity to the decamer probes. The adoption of the aqueous medium results in a 0.55 V potential positive shift, even after intersolvental normalization, of the peak related to the ET centered on the phthalimide ring (Figure S1). The complete loss of chemical reversibility of **P$_{Lys}$** appears consistent with both i) the proticity of water, accordingly with the above-described reversibility decrease of phthalimide signal upon proton additions in the DMF medium (Figure 3a), and ii) the appearance of a second shoulder-like reduction peak. According to former literature,[19,20] the latter could correspond to a second reduction step involving the hydroxyl radical formed in the chemical step following the first ET, which competes with back reoxidation of the starting molecule.

3.3 | In search of the best detection limit for the decamers

One of the desirable features for a marker is to be detected at the lowest possible concentration. As shown above, both markers, phthalimide and nitro-phthalimide, maintain a satisfactory intensity of the voltammetric signals when linked to the decamers, **P$_{Dec}$** and **NP$_{Dec}$**, compared with that of their "precursors" (i.e., lysine conjugate and free molecule). Aiming to improve the detectability of these chemical labels, two strategies have been applied: i) variation of the electrode material (GC vs. Hg), and ii) appli-

TABLE 1 Summary of the detection limit (DL) obtained for the six molecules studied, in different operating media and with different electrochemical techniques on the HDME electrode. Bold characters denote the best protocol for each molecule. The stripping results are obtained after a 60 s deposition time (for more information see Experimental Section)

Sample	Medium	Technique	DL (μmol/dm^3)
Diffusive techniques			
P	H$_2$O	CV	6
		DPV	**0.1**
		SWV	1
P$_{Lys}$	H$_2$O	CV	7
		DPV	3 (30)[a]
		SWV	**1**
P$_{Dec}$[b]	DMF	SWV	3
NP[b]	DMF	CV	6
		DPV	**0.6**
		SWV	6
NP$_{Lys}$[c]	DMF	CV	10
		DPV	**6.5**
		SWV	**6.5**
NP$_{Dec}$[b,c]	DMF	SWV	1–3
Stripping techniques			
P$_{Dec}$	H$_2$O	**Ad(T)-PSA**	**0.2–0.02**
NP$_{Dec}$	H$_2$O	**Ad(T)-PSA**	**0.2–0.02**

[a]The value in brackets is obtained using GC electrode, for sake of comparison.
[b]Only the SWV technique gives rise to suitable signals, probably due to the limited scale time of the measurement (compared to that of DPV) which minimizes adsorption phenomena negatively influencing the correlation signal-sample concentration.
[c]The DL is the best one obtained using one of the available peaks.

cation of different electrochemical techniques (differential vs. linear voltammetry; stripping vs. diffusive methods; potentiometry vs. voltammetry).

The results of this screening study are summarized in Table 1, while a detailed report of the experiments aimed at the estimation of the lowest detection limit (DL), together with verification of the linearity of the dynamic range in the concentration interval tested, is provided in the Supporting Information (Figures S2–S7).

Hg appears by far better than GC as a working electrode material, as it allows reaching lower detection limits for all the diffusive techniques implemented probably because of its smaller electrical capacity resulting in a higher signal-to-noise ratio. Other undoubted advantages of this material are its high H$_2$ overpotential, ensuring a broader cathodic window in water, as well as surface easy renewability (particularly in the case of filming processes). Among diffusive techniques, the most intense signals were obtained with the two differential pulse techniques,

DPV and SWV (Figure S8), as expected because of their capability to minimize the capacitive component in the recorded current with respect to the faradaic one (Table 1). The analytical response falls within the linear dynamic range for all the detected concentrations (except for both decamers) in terms of both peak heights and areas, albeit peak currents generally result in slightly better linearity (Figures S2–S7).

Both phthalimide-based markers offer comparable detection limits especially when conjugated with the PNA decamer. Nonetheless, the NP marker can claim at least two advantages with respect to the P one: *i*) more than one signal is available and *ii*) thanks to the electron attracting nitro group, such signals are located at less negative potentials than with simple phthalimide. In both the P and NP series the DLs appear to increase (by nearly the same quantities) with increasing steric hindrance (and, hence, decreasing diffusion coefficient) of the reacting molecule, moving from pristine markers to the corresponding labeled PNA decamers. However, it is worthwhile noticing that in both cases, a larger variation is observed between the free marker and the corresponding lysine conjugate than between the latter and the corresponding decamer conjugate, despite the much more significant increase in steric hindrance of the latter couple. This could point to some specific interaction of the nitrogen-rich PNA chain with the Hg surface, promoting/enhancing substrate adsorption and therefore pre-concentration even during the running of the diffusive techniques.

Actually, the diffusion techniques appear to suffer from several weak points concerning the decamer cases:

- the limit of detection is not that brilliant;
- in the **P$_{Dec}$** case the only exploitable signal is partly superimposed to the background (Figure S4), resulting in lower accuracy;
- the reproducibility of the peak currents is not satisfactory because of the already mentioned affinity of PNA decamers for the mercury surface, this requires a careful standardization of the time between sample addition and measurement in order to obtain reproducible data. This assumption is supported by the observation that in the very bulky and surface-affine decamer cases the Hg electrode response even deviates from linearity at the upper end of the explored concentration range, pointing to some surface saturation effect (Figures S4 and S7).

However, the same last feature, which makes reproducibility of diffusive analysis difficult, represents a strong point for the decamers, offering the possibility to pre-concentrate them in a reproducible way on the electrode surface and thus to significantly improve the DL by applying stripping techniques. As already mentioned, in this

**Chemistry
Europe**
European Chemical
Societies Publishing
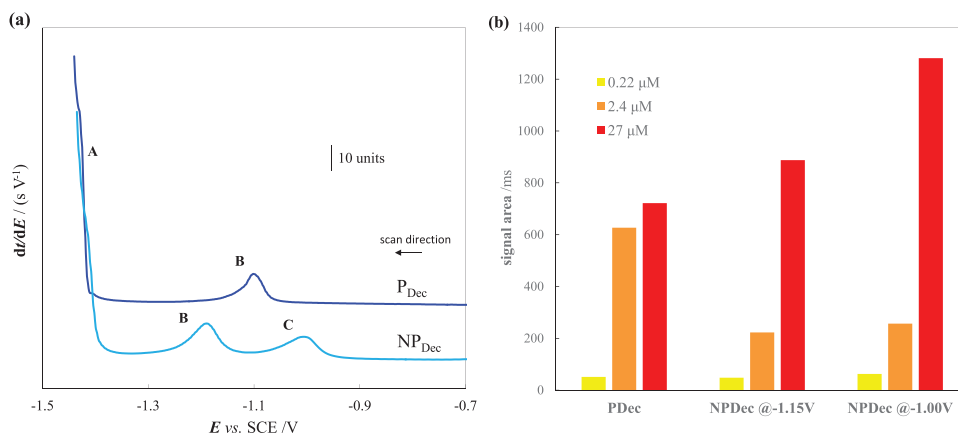
FIGURE 5   Left (a): Ad-PSA differential chronopotentiogram for P_{Dec} (top) and NP_{Dec} (bottom) at 27 μM concentration. Right (b): peak areas obtained at different concentrations of decamers (range from 10^{-9} to 10^{-5} M). All data are recorded on HDME in water with 0.2 M NaCl as supporting electrolyte and phosphate buffer (pH 7) 0.025 M. Experimental details: accumulation potential 0 V versus SCE in resting solution; 60 s accumulation time; 5 s equilibration time; −1 μA stripping current

work the pre-concentration step does not consist an electrodeposition (anodic or cathodic) but a pure adsorption phenomenon of the neutral PNA decamer backbone on the Hg surface. Assuming the same mechanism known for DNA,[10] nitrogen atoms on purinic and pyrimidinic rings of nucleobases play an important role in the surface interaction with Hg.
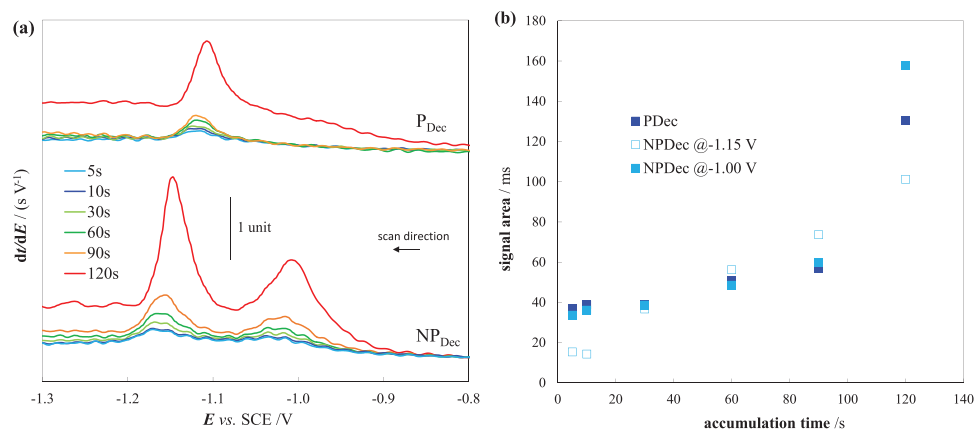
The classic stripping voltammetry techniques (square wave and differential pulse adsorptive stripping voltammetry, SW-AdSV and DP-AdSV) do not lead to significant improvements in the detection capability of minute amounts of either decamers, even after quite a long deposition time (i.e., 120 s). On the contrary, by giving up voltammetry as stripping step method, and resorting to the use of chronopotentiometry,[26,27] significant improvements are achieved in terms of both sensitivity and signal morphology. In fact, after differentiation of the recorded signal, Ad-PSA gives rise to well-defined peaks for both markers on a flat background signal (peak B for $\mathbf{P_{Dec}}$, peak B and C for $\mathbf{NP_{Dec}}$ in Figure 5a), well suitable for reliable quantitative analysis. As a result, Ad-PSA enables us to lower LODs to the 10^{-7} M range and even below for both the labeled PNA decamers (Table 1), i.e. one order of magnitude lower than free marker cases, the more remarkable considering the huge difference in steric hindrance between marker and PNA decamer. Looking at the adsorption isotherms (Figure 5b), obtained at constant accumulation conditions, $\mathbf{P_{Dec}}$ exhibits a more evident signal saturation, resembling a Langmuir-like type I isotherm,[28] contrary to the nitro-labeled analogous that shows a significant increase of the signal at the highest concentration (resembling a type III isotherm [28]).

Concerning the adsorption kinetics, an increase in the adsorption time (keeping constant experimental param-

eters, i.e., sample concentration, pH, stripping current) results in a peak area rise that does not show any surface saturation effect up to 120 s of accumulation (Figure 6). At the lower investigated concentration of 0.22 μM, both labeled PNAs behave similarly, with an invariable supralinear increase of the signal for the accumulation time of 120 s. When working at a concentration one order of magnitude higher, while a comparable adsorption rate is preserved for both PNA decamers, an invariably higher signal was detected for $\mathbf{P_{Dec}}$ (Figure S9).

The importance of the electroactive labeling of PNA is made evident by commenting on the features of the sole signal attributable to the redox activity of the peptide nucleic acid backbone. The latter, occurring at about −1.4 V versus SCE (peak A in Figure 5a) and attributed to the reduction of adenine and cytosine bases (likewise DNA studies[18]), is quite difficult to be quantitatively analyzed being superimposed on the background signal (Figure S10). Moreover, such a signal is detectable only for concentrations at least in the μM range.

Finally, the results obtained with Ad-PSA were compared with the transfer protocol AdT-PSA (Chart 1), which implies the pre-concentration and stripping stage being performed in two different solutions (analyte-containing and analyte-free ones, respectively).[13,18] A direct advantage of the AdT protocol, although more laborious, is that a small amount of PNA solution can be analyzed (i.e., 10 μl sample drop) and that the detection stage is performed in a fully aqueous matrix (i.e., 0.2 M NaCl buffered at pH 7) without any contamination by the DMF necessary for assuring the solubility of decamers in the Ad mode. AdT-PSA gives rise to chronopotentiograms very similar to the Ad-PSA ones, in terms of both positions (with a gap around 0.01–0.02 V) and intensities (Figure S11).

11 of 12 **Electrochemical Science Advances** RESEARCH ARTICLE
doi.org/10.1002/elsa.202100164

Chemistry
Europe
European Chemical
Societies Publishing

FIGURE 6 Left: Ad-PSA differential chronopotentiogram for P_{Dec} (top) and NP_{Dec} (bottom) at 0.22 μM concentration recorded at increasing accumulation time. Right: corresponding peak area values as a function of the accumulation time. Experimental conditions as reported in Figure 5

4 | CONCLUSIONS

Phthalimide and 4-nitrophthalimide were covalently bound to PNA decamers to act as new electroactive redox labels for the development of electrochemical biosensors for the detection of DNA/ RNA sequences. Both markers are promising, not only for their intrinsic features (e.g., being metal-free and offering easy synthetic accessibility for their linkage to PNA oligomers), but also for their electrochemical behavior that makes it possible a low detection limit that stands between 10 and 100 nM, hence making PNA quantities below the ppm level detectable, unto some tens of ppb. Both markers show comparably good performance as PNA labels, and both are exploitable for detection in water. However, the NP marker offers the additional advantage of the availability of two well-defined signals rather than a single one, with the first of them, related to the nitro group, located in a milder potential region.

Focusing on the detectability of the molecules:

- mercury (in the form of HDME) resulted in a more performing electrode material than GC because of i) its intrinsic lower electric capacity, which results in better signal-to-noise ratio, and ii) its surface affinity with nitrogen-rich molecules (like nucleotides), promoting or enhancing effective surface adsorption of the analytes;
- among diffusive voltammetric techniques, the best results were invariably obtained with differential techniques (SWV and DPV), but the detection limits for the decamers were not very attractive being at least one order of magnitude higher than the pristine markers;
- significant improvement of DLs for the two decamers, P_{Dec} and NP_{Dec}, was reached employing the PSA com-

bined with an adsorption pre-concentrating step, in both Adsorptive (Ad-PSA) and Adsorptive Transfer (AdT-PSA) versions. While AdT-PSA is experimentally quite more onerous, it enables to significantly reduce the amount of PNA solution (10 μl drop with respect to 3 ml for Ad-PSA) and to perform the analysis in a fully aqueous solution. The results obtained with the two protocols (e.g., signal position and intensity) are quite comparable.

In the present work, for sake of comparison between Ad- and AdT-PSA results, all pre-concentrations were carried out in stationary solutions as it was not easy to induce a forced convection into a small sample drop likewise for a batch solution. Nonetheless, the detection limit in PSA could be further improved inducing a forced convection into the sample solution during the first phase of pre-concentration.

In conclusion, the combination of Hg electrode with PSA technique seems to be a powerful electroanalytical method for the detection of DNA mimetic molecules. Even if the here reported detection limits for PNA molecules are not the lowest in literature, it must be underlined that no transition metal coordination compounds nor any sort of chemical signal amplification (such as catalysts or enzymes) were adopted that would have made the method less sustainable and/or more complex and expensive. As a result, good performance was obtained by merely exploiting electrode material features and electroanalytical technique potentialities in carefully optimized synergy. A further step forward in this field will be the identification of alternative electrode materials less toxic than mercury but with comparable electrochemical and adsorbing features. Taking inspiration from the innovative research in the field of stripping voltammetry, besides bismuth and

antimony (well-known alternative to Hg for the quantification of heavy metal cations), Authors tentatively propose gold (for its good adsorption properties towards sulfur and nitrogen-containing molecules) and the less known galinstan as potentially valuable alternatives. The latter is a eutectic mixture of Ga-In-Sn that shares with Hg both the liquid state and the high hydrogen overpotential. For the exploitation in combination with PNA/DNA oligomers, galinstan could be an optimal choice due to its proven adsorption capability towards various nitrogen-containing organic functional groups.[29]

CONFLICT OF INTEREST
The authors declare no conflict of interest.

DATA AVAILABILITY STATEMENT
The data that support the findings of this study are available from the corresponding author upon reasonable request.

ORCID
Mirko Magni https://orcid.org/0000-0001-9776-2973
Sergio Dall'Angelo https://orcid.org/0000-0001-9377-0474
Clara Baldoli https://orcid.org/0000-0001-5504-8624
Emanuela Licandro https://orcid.org/0000-0003-0168-9295
Luigi Falciola https://orcid.org/0000-0002-2031-239X
Patrizia R. Mussini https://orcid.org/0000-0003-4063-1563

REFERENCES
1. P. E. Nielsen, M. Egholm, R. H. Berg, O. Buchardt, *Science* **1991**, *254*, 1497.
2. M. Egholm, O. Buchardt, L. Christensen, C. Behrens, S. M. Freier, D. A. Driver, R. H. Berg, S. K. Kim, B. Norden, P. E. Nielsen, *Nature* **1993**, *365*, 566.
3. J. Saarbach, P. M. Sabale, N. Winssinger, *Curr. Opin. Chem. Biol.* **2019**, *52*, 112.
4. S. Shakeel, S. Karim, A. Ali, *J. Chem. Technol. Biotechnol.* **2006**, *81*, 892.
5. N. Zhang, D. H. Appella, *J. Infect. Dis.* **2010**, *201*, S42.
6. Q. Lai, W. Chen, Y. Zhang, Z.-C. Liu, *Analyst* **2021**, *146*, 5822.
7. H. Sun, J. Kong, X. Zhang, *Biopolymers* **2021**, *112*.
8. M. Moccia, V. Caratelli, S. Cinti, B. Pede, C. Avitabile, M. Saviano, A. L. Imbriani, D. Moscone, F. Arduini, *Biosensors and Bioelectronics* **2020**, *165*, 112371.
9. C. Baldoli, E. Licandro, S. Maiorana, D. Resemini, C. Rigamonti, L. Falciola, M. Longhi, P.R. Mussini, *J. Electroanal. Chem.* **2005**, *585*, 197.
10. E. Paleček, *Bioelectrochem. Bioenerg.* **1988**, *20*, 179.
11. M. Fojta, V. Vetterl, M. Tomschik, F. Jelen, P. Nielsen, J. Wang, E. Paleček, *Biophys. J.* **1997**, *72*, 2285.
12. E. Paleček, M. Trefulka, M. Fojta, *Electroch. Comm.* **2009**, *11*, 359.
13. E. Paleček, *Anal. Biochem.* **1988**, *170*, 421.
14. J. Wang, *Analytical Electrochemistry*, 2nd ed., Wiley, New York **2000**.
15. J. M. Estela, C. Tomás, A. Cladera, V. Cerdà, *Crit. Rev. Anal. Chem.* **1995**, *25*, 91.
16. P. E. Nielsen, *Peptide Nucleic Acids: Protocols and Applications*, 2nd ed., Horizon Bioscience, Wymondham (UK) **2004**.
17. G. Gritzner, J. Kuta, *Pure Appl. Chem.* **1984**, *56*, 461.
18. E. Paleček, F. Jelen, C. Teijeiro, V. Fučik, T.M. Jovin, *Anal. Chim. Acta* **1993**, *273*, 175.
19. D. W. Leedy, D. L. Muck, *J. Am. Chem. Soc.* **1971**, *93*, 4264.
20. G. Farnia, A. Romanin, G. Capobianco, F. Torzo, *J. Electroanal. Chem.* **1971**, *33*, 31.
21. C. Hansch, A. Leo, R.W. Taft, *Chem. Rev.* **1991**, *91*, 165.
22. C. Amatore, in *Organic Electrochemistry Revised and Expanded*, 4th ed. (Eds: Henning Lund, Ole Hammerich), New York **2001**, pp. 3–96.
23. J.-M. Saveant, *Elements of Molecular and Biomolecular Electrochemistry*, Wiley, New Jersey **2006**.
24. B. S. Jensen, V. D. Parker, *J. Chem. Soc., Chem. Comm.* **1974**, *10*, 367.
25. S. H. Cadle, P. R. Tice, J. Q. Chamber, *J. Phys. Chem.* **1967**, *71*, 3517.
26. J. Wang, G. Rivas, X. Cai, M. Chicharro, N. Dontha, D. Luo, E. Palecek, P. Nielsen, *Electroanalysis* **1997**, *9*, 120.
27. J. Wang, D.H. Grant, M. Ozsoz, X. Cai, B. Tian, J.R. Fernandes, *Anal. Chim. Acta* **1997**, *349*, 77.
28. M. A. Al-Ghouti, D. A. Da'ana, *J. Hazard. Mater.* **2020**, *393*, 122383.
29. H. Channaa, P. Surmann, *Pharmazie* **2009**, *64*, 161.

SUPPORTING INFORMATION
Additional supporting information may be found in the online version of the article at the publisher's website.